

Original Investigation

Enhancing Preoperative Diagnosis of Subscapular Muscle Injuries with Shoulder MRI-based Multimodal Radiomics

Zexing He¹, Kaibin Fang¹, Xiaocong Lin, ChengHao Xiang, Yuanzhe Li, Nianlai Huang, XuJun Hu, Zekai Chen, Zhangsheng Dai²

Rationale and Objectives: Rotator cuff injury is a common ailment in the musculoskeletal system, with the subscapularis muscle being the largest and most robust muscle of the rotator cuff. The occurrence of subscapularis muscle tears is more frequent than previously reported. The main objective of this research is to harness the power of artificial intelligence to enhance the precision in diagnosing subscapularis muscle injuries via magnetic resonance imaging of the shoulder joint, prior to surgical intervention. This study seeks to integrate advanced artificial intelligence algorithms to analyze magnetic resonance imaging data, aiming to provide more accurate preoperative assessments, which can potentially lead to better surgical outcomes and patient care and promote technological progress in the field of medical imaging analysis.

Method: This is a multicenter study that involves 324 patients from a major medical center serving as both the training and testing groups, with an additional 60 patients from two other medical centers comprising the verifying group. The imaging protocol for all these subjects included a series of shoulder magnetic resonance imaging scans: T1-weighted coronal sequences, T2-weighted coronal, axial, and sagittal images. These comprehensive imaging modalities were utilized to thoroughly examine the shoulder joint's anatomical details and to detect any signs of subscapularis muscle damage. To enhance the diagnostic accuracy before surgical procedures, radiomic analysis was employed. This technique involves the extraction of a multitude of quantitative features from the magnetic resonance imaging, which can provide a more nuanced and data-driven approach to identifying subscapularis muscle injuries. The integration of radiomics in this study aims to offer a more precise preoperative assessment, potentially leading to improved surgical planning and patient outcomes.

Result: In the course of this study, a comprehensive extraction of 1197 radiomic features was performed for each imaging modality of every patient. The coronal T1-weighted modality, when assessed within the internal verifying cohort, delivered a diagnostic accuracy of 0.766, coupled with an AUC of 0.803. In the case of the T2-weighted modality, the coronal planes exhibited a diagnostic accuracy of 0.781 and an AUC of 0.844. The axial T2-weighted images recorded an accuracy of 0.719 and an AUC of 0.761, while the sagittal T2-weighted images scored an accuracy of 0.766 and an AUC of 0.821. The amalgamation of these imaging techniques through a multimodal strategy markedly enhanced the accuracy to 0.828, with an AUC of 0.916 for the internal verifying group. The diagnostic performance of the coronal T1-weighted modality in the external verifying cohort yielded an accuracy of 0.833, with an area under the curve (AUC) of 0.819. For the T2-weighted modality, the coronal imaging demonstrated an accuracy of 0.767 and an AUC of 0.794. The axial T2-weighted images had an accuracy of 0.783 and an AUC of 0.797, while the sagittal T2-weighted images achieved an accuracy of 0.833 and an AUC of 0.800. When combining the modalities, the multimodal approach significantly improved the accuracy to 0.867, with an AUC of 0.803 in the external verifying group, indicating a robust diagnostic capability.

Conclusion: Our study demonstrates that the application of multimodal radiomic techniques to shoulder magnetic resonance imaging significantly enhances the precision of preoperative diagnosis for subscapularis muscle injuries. This approach leverages the comprehensive data provided by various magnetic resonance imaging modalities to offer a more detailed and accurate assessment, which is crucial for surgical planning and patient care.

Acad Radiol xxxx; xx:xxxx-xxx

From the Department of Orthopaedic Surgery, The Second Affiliated Hospital of Fujian Medical University, Quanzhou 362000, China (Z.H., K.F., X.L., N.H., Z.D.); Department of Joint Surgery, The Central Hospital of Enshi Tujia and Miao Autonomous Prefecture, Enshi 445000, China (C.X.); Department of CT/MRI, The Second Affiliated Hospital of Fujian Medical University, Quanzhou 362000, China (Y.L.); Department of Orthopaedic Surgery, Shaoxing People's Hospital, Shaoxing 312300, China (X.H.); Department of clinical medicine, School of Basic Medicine, Fujian Medical University, Fuzhou 350108, China (Z.C.). Received July 1, 2024; revised September 23, 2024; accepted September 23, 2024. **Address correspondence to:** Z.D. e-mail: 1009828183@qq.com

¹ Zexing He and Kaibin Fang contributed equally to this work.

² These authors contributed equally to this work.

© 2024 The Association of University Radiologists. Published by Elsevier Inc. This is an open access article under the CC BY-NC-ND license (<http://creativecommons.org/licenses/by-nc-nd/4.0/>).

<https://doi.org/10.1016/j.acra.2024.09.049>

Key Words: Shoulder magnetic resonance imaging; Radiomics; Multimodal; Subscapularis; Injury.

© 2024 The Association of University Radiologists. Published by Elsevier Inc. This is an open access article under the CC BY-NC-ND license (<http://creativecommons.org/licenses/by-nc-nd/4.0/>).

Abbreviation: **MRI** Magnetic Resonance Imaging, **COR** Coronal, **AXI** Axial, **SAG** Sagittal, **SMI** Subscapularis muscle Injury, **NSM** Normal Subscapularis muscle, **ROI** Regions of interest, **ICC** intraclass correlation coefficient, **AUC** Area Under the Curve, **RF** Random Forest, **DCA** Decision Curve Analysis

BACKGROUND

The subscapularis is the largest and most powerful of the rotator cuff muscles and fulfills an important role in glenohumeral movement and stability. The spectrum and implications of subscapularis muscle or tendon injury differ from injury to other rotator cuff components because of its unique structure and function. Diagnosing subscapularis injury is clinically difficult and assessment of subscapularis integrity may be limited during arthroscopy or open surgery. Diagnostic imaging plays an important part in diagnosing and evaluating the extent of subscapularis injury (1). Magnetic resonance imaging (MRI) is valuable for assessing the extent and nature of rotator cuff pathology. MRI can provide accurate details about cuff tears, including partial or full-thickness, as well as their size, location, and degree of retraction (2).

If a subscapularis tendon rupture is suspected in the initial clinical testing, the primary diagnostics should include cross-sectional magnetic resonance imaging to assess the tendon lesion and to detect concomitant pathologies. Nevertheless, subscapularis tendon lesions are often initially overlooked and first correctly diagnosed during shoulder arthroscopy (3).

Although arthroscopy can more clearly distinguish injuries to the subscapularis muscle, not all injuries can be detected. Even cases with full-thickness tears of the subscapularis tendon that were completely detached from the footprint could be overlooked because of undetected retraction of the torn tendon or concealment by the superior glenohumeral ligament. Among revision rotator cuff repairs, 43.1% had neglected subscapularis tears, and fatty infiltration of these initially neglected subscapularis tendons showed further progression at the time of revision. The retear rate after the repair of neglected subscapularis tears was higher than expected. Thus, detecting and treating subscapularis tear via meticulous preoperative evaluation and thorough inspection during primary arthroscopy are essential (4). Radiomics technology is a practical tool for evaluating the integrity of the subscapularis muscle.

Radiomics involves extracting actionable data from medical images and analyzing it to aid in diagnosis, predict prognosis, and provide clinical decision support, all with the aim of advancing precision medicine (5).

In this study, the authors attempted to use multimodal radiomics techniques based on shoulder magnetic resonance imaging for preoperative diagnosis of subscapular muscle injury.

MATERIALS AND METHODS

This retrospective study meticulously analyzed the clinical symptoms of adult patients who received shoulder MRI scans in three large hospitals between January 2023 and January 2024. These imaging assessments were conducted prior to surgical procedures, and the study included a review of intraoperative findings documented in the medical records of patients with subscapularis muscle injuries. The study excluded individuals with a history of shoulder surgery, imaging artifacts that could compromise radiomic feature extraction, juveniles, and patients with associated fractures. The research was granted ethical approval by the hospital's Institutional Review Committee and was conducted in compliance.

A total of 324 patients from a large medical center were chosen for the training and testing group, while 60 patients from two other medical centers were selected for the verifying group. During the training and testing phase, there were 105 patients diagnosed with subscapularis muscle injury (SMI) and 219 patients with normal subscapularis muscle (NSM). In the verifying group, there were 25 patients with subscapularis muscle injury and 35 patients with normal subscapularis muscle. The patient inclusion process is shown in Figure 1.

Image Preprocessing

The selection of the region of interest (ROI) was meticulously tailored to encompass four distinct MRI views of the shoulder: coronal T1-weighted, coronal T2-weighted, axial T2-weighted, and sagittal T2-weighted images. The reconstruction of images and the precise delineation of the region of interest (ROI) were executed utilizing the ITK SNAP software (6). When delineating the region of interest (ROI), we encountered a challenge with certain patients who exhibited rupture and retraction of the subscapular tendon, which obscured the clear identification of the actual boundary. To address this issue, we opted for a comprehensive depiction of the subscapular muscle in these patients, encompassing the full extent from the subscapular fossa to the humeral small tuberosity. This approach ensures a thorough representation of the subscapularis tendon. The process of outlining ROI is shown in Figure 2.

The delineation of the region of interest (ROI) was performed by an orthopedic sports medicine physician with specialized knowledge, and the radiologist were responsible



Figure 1. The process of patient inclusion.

for quality control of the results. To quantify the consistency in the evaluation of subscapularis muscle injuries and normal states, the intraclass correlation coefficient (ICC) was employed as a statistical measure. Initially, one researcher delineated the ROI, and then a colleague used a dataset of 384 cases with predefined ROIs to calculate the ICC, thus assessing the uniformity of the delineation process. The criterion for advancing to radiomic feature analysis is that all ICC values within the dataset must surpass a value of 0.9, indicating a high level of agreement in the ROI identification.

Radiomics Feature Extraction

The feature extraction process was carried out using the Pyradiomics Module (<https://github.com/Radiomics/pyradiomics>). A multitude of image filters, including the Laplacian of Gaussian and wavelet techniques, were strategically employed to broaden the spectrum of derived images, thereby enriching the feature extraction process. All radiomic features were categorized into seven groups: shape-based features, first-order features, gray-level dependence matrix (GLDM) features, gray-level size zone matrix (GLSZM) features, neighboring gray-tone difference matrix (NGTDM) features, gray-level run-length matrix (GLRLM) features, and gray-level co-occurrence matrix (GLCM) features.

Feature Selection

In order to identify the most relevant features associated with the subscapularis injury, a meticulous feature selection process was implemented. The data was initially archived in CSV format, with annotated datasets consolidated to form the training dataset. Regularization was applied using the Z-test, followed by feature screening through the t-test with a significance level of $p < 0.05$. To ensure the selection of statistically robust features, any with intraclass correlation (ICC) coefficients below 0.9 were omitted. This meticulous process significantly reduced feature count while preserving their predictive efficacy. To mitigate multicollinearity, a Pearson correlation analysis was conducted to scrutinize inter-feature relationships. Correlation coefficients were calculated to pinpoint feature pairs with values of ≥ 0.9 or ≤ -0.9 . In instances of high correlation, only the feature with

superior diagnostic efficacy was retained, thus avoiding redundancy. The method of minimum redundancy and maximum correlation (mRMR) was applied to identify the 20 most significant features from the given set of features (7). To further refine the feature set, the least absolute shrinkage and selection operator(LASSO) logistic regression technique was employed (8). Perform unimodal analyses by extracting 6, 9, 10, and 10 features from T1COR, T2COR, T2AXI, and T2SAG images, respectively. After the screening process, 3 radiomic features based on coronal T1-weighted images, 1 radiomic feature based on coronal T2-weighted images, 3 radiomic features based on axial T2-weighted images, and 3 radiomic features based on sagittal T2-weighted images are selected. A pre-fusion method is employed to integrate the radiomic features extracted from both T1-weighted and T2-weighted phases for a multimodal analysis. A preliminary model selection was made based on the filtered data, followed by cross-validation with a specified number of iterations, utilizing a zoning strategy, 80% of the 324 patients at the first hospital were assigned to training, the remaining 20% to testing, and data from a total of 60 patients at the other two hospitals were used to validate the results.

Machine Learning Models

For the analysis, the random forest was chosen as the radiomics feature selector. Random Forests(RF), an ensemble method based on classification and regression trees trained on bootstrapped samples and randomly selected features, has been shown to have superior performance over many other classification and regression methods (9). It is a nonparametric approach that can accommodate different types of responses. Moreover, it can work with predictors of various scales or distributions and is suited for applications in high-dimensional settings where the number of predictors can be larger than the number of observations. Thus, it is very suitable for analyzing complex data which are often high-dimensional (10).

Statistical Analysis

For the analysis, leverage Python-based statistical libraries such as Statsmodels, NumPy, Pandas, and SciPy. Decision curve analysis(DCA) is a novel method for evaluating diagnostic tests, prediction models and molecular markers. It

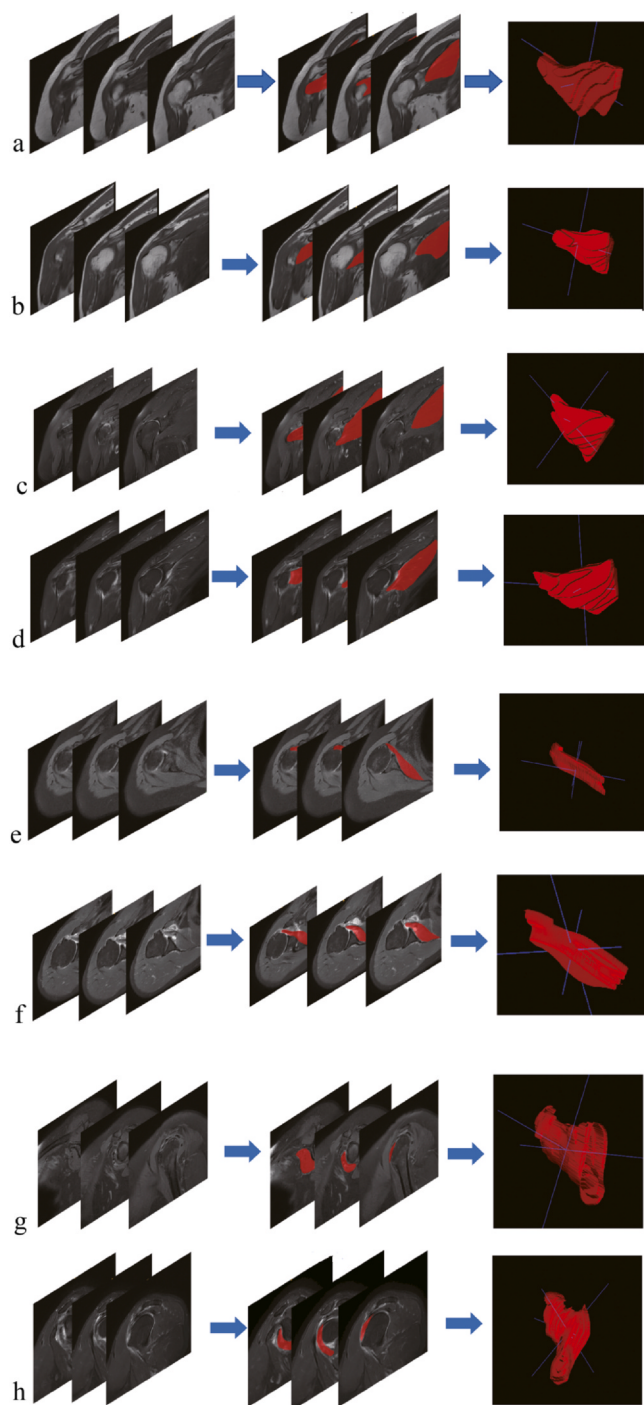


Figure 2. The process of outlining ROI. (a) Coronal T1-weighted of NSM. (b) Coronal T1-weighted of SMI. (c) Coronal T2-weighted of NSM. (d) Coronal T2-weighted of SMI. (e) Axial T2-weighted of NSM. (f) Axial T2-weighted of SMI. (g) Sagittal T2-weighted of NSM. (h) Sagittal T2-weighted of SMI.

combines the mathematical simplicity of accuracy measures, such as sensitivity and specificity, with the clinical applicability of decision analytic approaches (11). If a model's DCA curve is above another model at all thresholds, then this model has better clinical utility. The DCA curve provides an intuitive way to evaluate the utility of predictive models in

actual clinical settings. The DCA curve can also help doctors make more personalized treatment decisions based on the individual risk preferences of patients. Assess the predictive model's efficacy by calculating the Area Under the Curve (AUC) and determine the 95% confidence interval (CI) of the AUC using the bootstrap method with 1000 resampling intervals (12). To comparatively evaluate the AUC across various models, employ the DeLong test to statistically gauge the divergence in performance metrics between them (13).

RESULTS

Radiomics Feature Extraction

1197 radiomics features were extracted for each modality of each patient. Among them, there are 936 features of the firstorder type, 1144 features of the glcm type, 728 features of the gldm type, 832 features of the glrlm type, 832 features of the glszm type, 260 features of the ngtdm type, and 56 features of the shape type.

Exploring the Diagnostic Value of Radiomic Features Extracted from T1-Weighted Shoulder MRI for Identifying SMI versus NSM

Following a rigorous selection process, 6 radiomic features derived from coronal T1-weighted MRI images of the shoulder were identified. These features demonstrated an accuracy of 0.823 in the training cohort for differentiating between SMI and NSM, with an AUC of 0.866. During the internal verifying cohort consisted of the testing cohort, the accuracy of these features for the same differentiation was 0.766, yielding an AUC of 0.803. In the external verifying phase, the accuracy of these features for the same differentiation was 0.833, yielding an AUC of 0.819. The efficacy of utilizing T1-weighted radiomic features to distinguish between SMI and NSM is illustrated in Figure 3 and detailed in Table 1.

Exploring the Diagnostic Value of Radiomic Features Extracted from T2-Weighted Shoulder MRI for Identifying SMI versus NSM

After screening, 9 radiomics features based on coronal T2 weighted images of shoulder magnetic resonance imaging were extracted. The accuracy of utilizing these features to differentiate between SMI and NSM in the training group is 0.762, AUC is 0.843. The accuracy of using these features to distinguish SMI and NSM in the internal verifying group is 0.781, AUC is 0.844. In the external verifying phase, the accuracy of these features for the same differentiation was 0.767, yielding an AUC of 0.794. The effectiveness of using radiomics features based on T2 weighted phase to distinguish SMI and NSM is shown in Figure 4 and Table 1.

After screening, 10 radiomics features based on axial T2 weighted images of shoulder magnetic resonance imaging were extracted. The accuracy of utilizing these features to

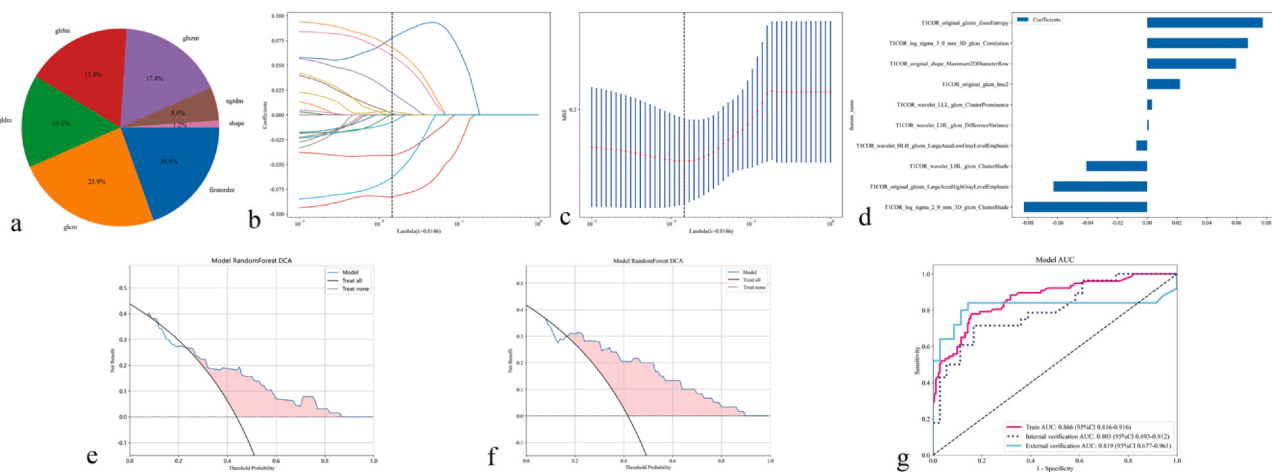


Figure 3. The effectiveness of the coronal T1 modal. (a) Extracted radiomics features. (b&c), using radiometric methods such as LASSO regression for feature screening. (d) Selected features. (e) Use RF machine learning models and filtered features to distinguish the DCA curves of SMI and NSM in the internal verifying group. (f) Use RF machine learning models and filtered features to differentiate the DCA curves of SMI and NSM in the external verifying group. (g) Use RF machine learning models and filtered features to distinguish the AUC curves of SMI and NSM.

differentiate between SMI and NSM in train group is 0.796, AUC is 0.892. The accuracy of using these features to distinguish SMI and NSM in the internal verifying group is 0.719, AUC is 0.761. In the external verifying phase, the accuracy of these features for the same differentiation was 0.783, yielding an AUC of 0.797. The effectiveness of using radiomics features based on T2 weighted phase to distinguish SMI and NSM is shown in Figure 5 and Table 1.

After screening, 10 radiomics features based on sagittal T2 weighted images of shoulder magnetic resonance imaging were extracted. The accuracy of utilizing these features to differentiate between SMI and NSM in train group is 0.827, AUC is 0.897. The accuracy of using these features to distinguish SMI and NSM in the internal verifying group is 0.766, AUC is 0.821. In the external verifying phase, the accuracy of these features for the same differentiation was 0.833, yielding an AUC of 0.800. The effectiveness of using radiomics features based on T2 weighted phase to distinguish SMI and NSM is shown in Figure 6 and Table 1.

Exploring the Diagnostic Value of Radiomic Features Extracted from T1-Weighted+T2-Weighted Shoulder MRI for Identifying SMI versus NSM

The pre-fusion method was employed to integrate radiomics features extracted from both the T1-weighted and T2-weighted phases. This process entailed the consolidation of 1197 distinctive features from each imaging orientation—coronal T1-weighted, coronal T2-weighted, axial T2-weighted, and sagittal T2-weighted—resulting in an extensive dataset of 4788 features. After screening, 3 radiomics features based on coronal T1 weighted images, 1 radiomics features based on coronal T2 weighted images, 3 radiomics features based on axial T2 weighted images and 3 radiomics features based on sagittal T2 weighted images were extracted. These selected features demonstrated a high

level of correctness, with an accuracy of 0.854 and an AUC of 0.925 in the training group for differentiating between SMI and NSM. In the internal verifying group, the features maintained robust performance, with an accuracy of 0.828 and an AUC of 0.916. In the external verifying phase, the accuracy of these features for the same differentiation was 0.867, yielding an AUC of 0.803. The effectiveness of using radiomics features based on multimodal weighted phase to distinguish SMI and NSM is shown in Figure 7 and Table 1.

Contrast Analysis of Effectiveness

The DeLong test was utilized to compare the Area Under the Curve (AUC) of the T1, T2, and combined multimodal modalities for their ability to differentiate between SMI and NSM. Comparative analysis revealed that, In the training group and internal verifying group, the AUC curves of multimodal and unimodal were compared by the Delong test, and the test results that were statistically significant ($p < 0.05$), indicating the superiority of multimodal in the training and internal verifying stages. However, in the external verifying phase, the DeLong test did not reveal any statistically significant differences between the AUC values of multimodal and unimodal. The DeLong test results are presented in Table 2.

DISCUSSION

In our research, the conclusive multimodal model, encompassing T1 and T2 modalities, exhibited an accuracy of 0.828 and an AUC value of 0.916 in discriminating between subscapularis muscle injury and normal subscapularis muscle within the internal verifying group, and an accuracy of 0.867 with an AUC value of 0.803 in the external verifying group. This discovery suggests that multimodal radiomics

TABLE 1. The Efficacy of Multimodal Radiomics Techniques in Distinguishing Subscapularis Muscle Injury and Normal Subscapularis Muscle

model_name	Accuracy	AUC	95% CI	Sensitivity	Specificity	PPV	NPV	Precision	Recall	F1	Threshold	Task
T1COR	0.823	0.866	0.8165 - 0.9162	0.766	0.847	0.678	0.896	0.678	0.766	0.720	0.315	Train
T1COR	0.766	0.803	0.6930 - 0.9121	0.679	0.833	0.760	0.769	0.679	0.717	0.717	0.220	InternalVerification
T1COR	0.833	0.819	0.6770 - 0.9608	0.800	0.857	0.800	0.857	0.800	0.800	0.800	0.227	ExternalVerification
T2COR	0.762	0.843	0.7913 - 0.8940	0.766	0.760	0.573	0.885	0.573	0.766	0.656	0.314	Train
T2COR	0.781	0.844	0.7500 - 0.9375	0.786	0.778	0.733	0.824	0.733	0.786	0.759	0.294	InternalVerification
T2COR	0.767	0.794	0.6685 - 0.9201	0.640	0.857	0.762	0.769	0.762	0.640	0.640	0.300	ExternalVerification
T2AXI	0.796	0.892	0.8478 - 0.9354	0.844	0.776	0.613	0.922	0.613	0.844	0.710	0.304	Train
T2AXI	0.719	0.761	0.6390 - 0.8838	0.536	0.861	0.750	0.705	0.750	0.536	0.625	0.316	InternalVerification
T2AXI	0.783	0.797	0.6735 - 0.9196	0.560	0.943	0.875	0.750	0.875	0.560	0.683	0.394	ExternalVerification
T2SAG	0.827	0.897	0.8593 - 0.9354	0.818	0.831	0.670	0.916	0.670	0.818	0.737	0.343	Train
T2SAG	0.766	0.821	0.7142 - 0.9277	0.536	0.944	0.882	0.723	0.882	0.536	0.667	0.332	InternalVerification
T2SAG	0.833	0.800	0.6573 - 0.9427	0.600	1.000	1.000	0.778	1.000	0.600	0.750	0.408	ExternalVerification
Multimodal	0.854	0.925	0.8907 - 0.9553	0.831	0.863	0.719	0.924	0.719	0.831	0.771	0.314	Train
Multimodal	0.828	0.916	0.8492 - 0.9831	0.786	0.861	0.815	0.838	0.815	0.786	0.800	0.204	InternalVerification
Multimodal	0.867	0.803	0.6519 - 0.9550	0.760	0.943	0.905	0.846	0.905	0.760	0.826	0.297	ExternalVerification

techniques using shoulder magnetic resonance imaging have the potential to early identify patients with subscapular muscle injuries. This finding also lays a research foundation for the application of radiomics techniques in subscapularis muscle injury diagnostics.

MR imaging is the standard diagnostic modality that provides a comprehensive and accurate assessment for both osseous and soft-tissue pathologic conditions of the shoulder (14). However, due to patient and technical reasons during the examination process, the imaging results were not satisfactory. Patient factors include claustrophobia and the lack of positioning constraints. Technical considerations include dynamic and real-time assessment, absence of contraindications due to implants, decreased cost, and portability (15).

In addition, a consistent finding is that larger subscapularis tendon tears are more easily detected using MRI scans whereas smaller tears are more frequently missed (16). This means that it is difficult to diagnose atypical subscapular muscle injuries using methods other than arthroscopy. AI-driven solutions improve diagnostic accuracy and have the potential to influence treatment planning and postoperative outcomes through the automated RCTs analysis of medical imaging (17).

A biomarker framework grounded in radiomic analysis of shoulder MRI has been specifically tailored for the diagnosis of subscapularis injuries. This innovative approach has significantly bolstered the accuracy of preoperative diagnostics, delivering significant results. Furthermore, the biomarkers derived from this radiomic analysis serve as a pivotal asset in the clinical decision-making landscape, facilitating more informed and precise treatment strategies.

This research acknowledges certain limitations that warrant attention. During the delineation of the Region of Interest (ROI), our approach encompassed the entire subscapularis muscle rather than focusing solely on the tendon. This comprehensive strategy was necessitated by the fact that patients with subscapularis muscle injuries often suffer from tendon rupture and retraction, which obscures the tendon's margins and precludes precise identification. Consequently, we performed a detailed feature analysis and extraction across the full extent of the subscapularis muscle. It is acknowledged that this holistic method could introduce some degree of error into the analytical outcomes, but the results are still worth referring to. Although this study is a multi-center validation study, the limited sample size may not provide extensive statistical support for the research results, thereby affecting the generalizability of the conclusions. Moreover, during the external verifying phase, the accuracy of multimodal data has increased, but it did not gain an advantage in AUC, and the single modality also has a certain effectiveness. There are two main reasons for this phenomenon. First, in the SHAP distribution of all samples in the multimodal model, the T2SAG samples had a significant impact on the model output process, causing the AUC of the multimodal to be biased towards T2SAG. On the other hand, the

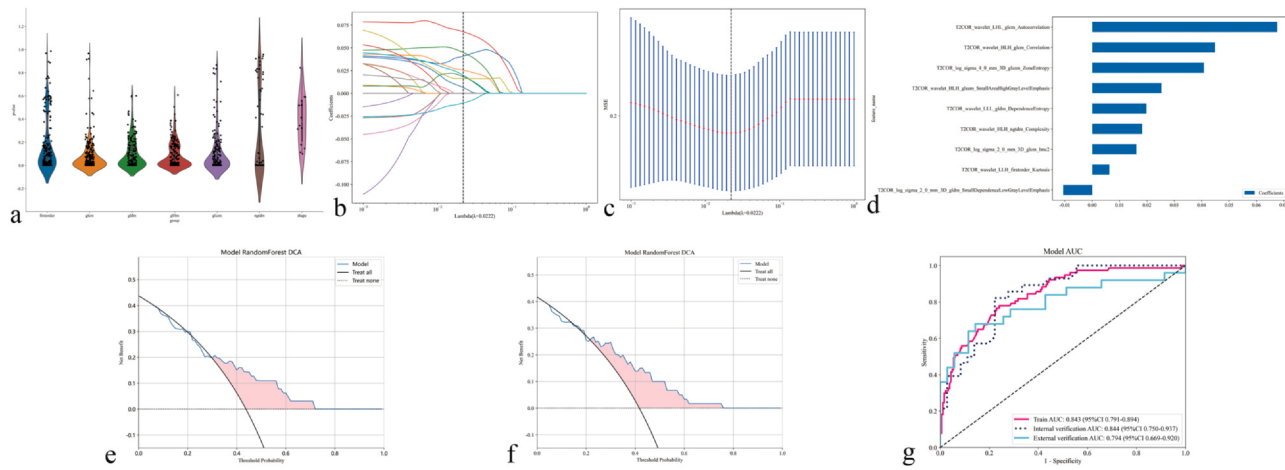


Figure 4. The effectiveness of the coronal T2 modal. (a) Extracted radiomics features. (b&c) using radiometric methods such as LASSO regression for feature screening. (d) Selected features. (e) Use RF machine learning models and filtered features to distinguish the DCA curves of SMI and NSM in the internal verifying group. (f) Use RF machine learning models and filtered features to differentiate the DCA curves of SMI and NSM in the external verifying group. (g) Use RF machine learning models and filtered features to distinguish the AUC curves of SMI and NSM.

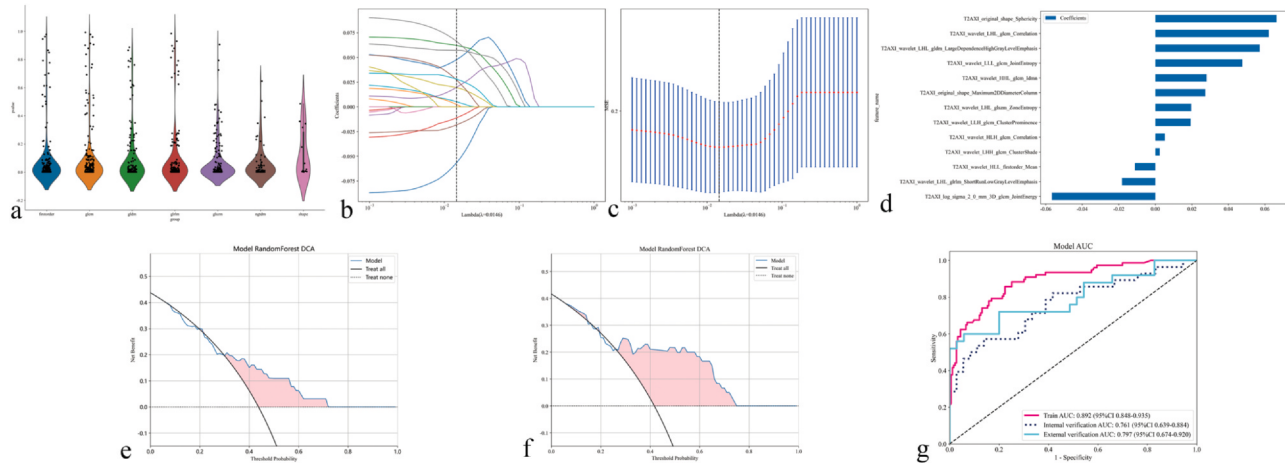


Figure 5. The effectiveness of the axial T2 modal. (a) Extracted radiomics features. (b&c) using radiometric methods such as LASSO regression for feature screening. (d) Selected features. (e) Use RF machine learning models and filtered features to distinguish the DCA curves of SMI and NSM in the internal verifying group. (f) Use RF machine learning models and filtered features to differentiate the DCA curves of SMI and NSM in the external verifying group. (g) Use RF machine learning models and filtered features to distinguish the AUC curves of SMI and NSM.

external validation data comes from two other hospitals, and the image features produced by different MRI devices are also different, causing the multimodal to lose its advantage in the external validation phase. However, multimodal is easy to obtain and has a high accuracy, so multimodal has a certain advantage in diagnosing subscapularis muscle injuries.

The multimodal radiomics technology, derived from shoulder MRI, has achieved promising preliminary advances in the diagnosis of subscapular muscle injuries. Nowadays, the preoperative diagnosis of subscapularis muscle injuries primarily relies on radiologists' interpretation of magnetic resonance images, which is not only time-consuming and labor-intensive but also carries the risk of missed diagnoses. Multimodal radiomics technology,

facilitated by artificial intelligence, can identify subscapularis muscle injuries swiftly and accurately. Compared to single-modality radiomics, it provides additional information to physicians, assisting them in making more precise treatment decisions, including the formulation of personalized treatment plans. With the ongoing refinement and evolution of this technology, it is poised to emerge as a valuable diagnostic asset in the medical field. Additionally, the ROI analysis in this study employs a combination of manual and semi-automated techniques. It is suggested that future endeavors could investigate the implementation of a fully automated approach, particularly with the benefit of a more substantial sample size, to augment the accuracy and efficiency of the analytical process.

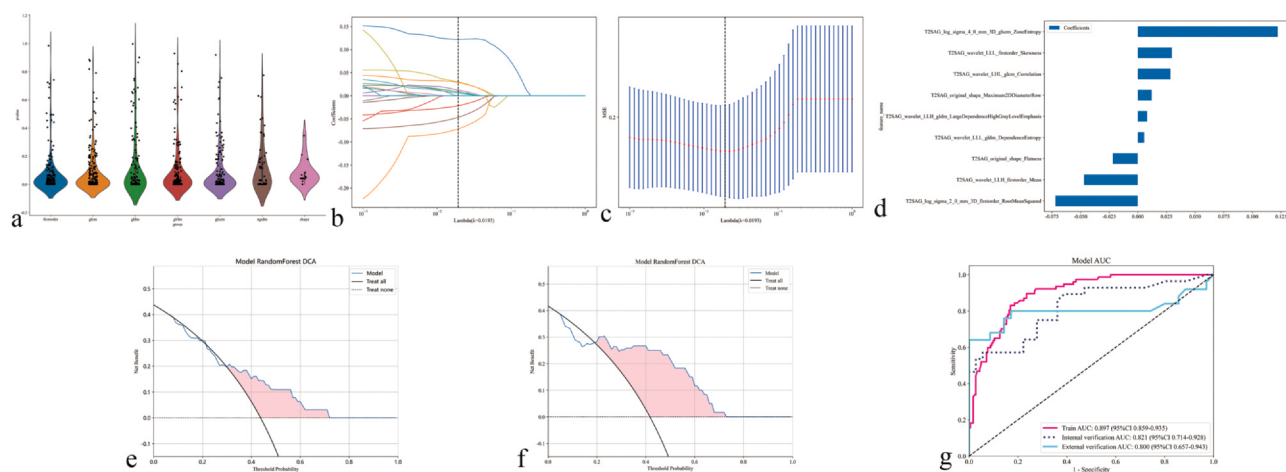


Figure 6. The effectiveness of the sagittal T2 modal. (a) Extracted radiomics features. (b&c) using radiometric methods such as LASSO regression for feature screening. (d) Selected features. (e) Use RF machine learning models and filtered features to distinguish the DCA curves of SMI and NSM in the internal verifying group. (f) Use RF machine learning models and filtered features to differentiate the DCA curves of SMI and NSM in the external verifying group. (g) Use RF machine learning models and filtered features to distinguish the AUC curves of SMI and NSM.

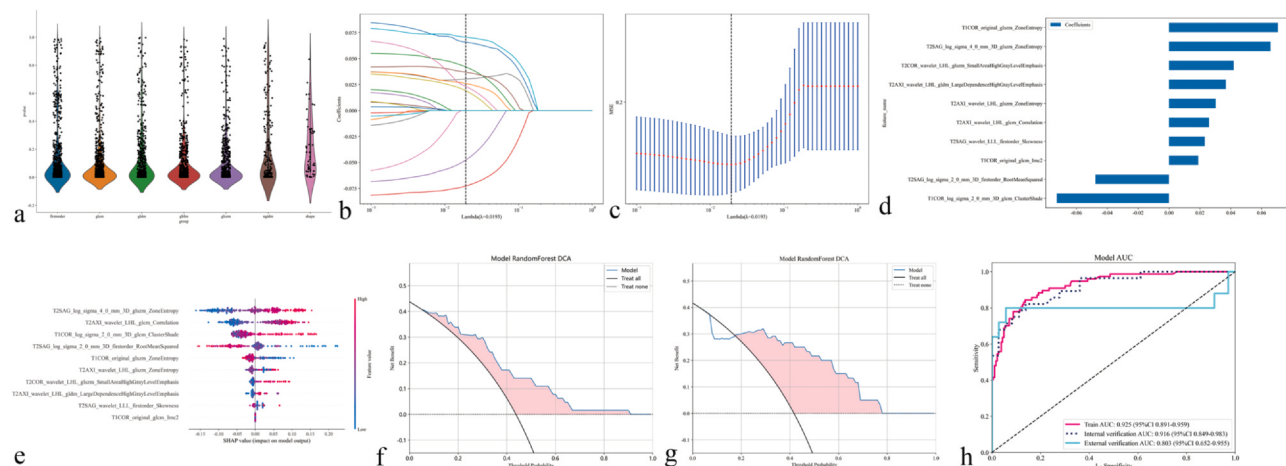


Figure 7. The effectiveness of the Multimodal modal. (a) Extracted radiomics features. (b&c), using radiometric methods such as LASSO regression for feature screening. (d) Selected features. (e) SHAP distribution of all samples in the model. (f) Use RF machine learning models and filtered features to distinguish the DCA curves of SMI and NSM in the internal verifying group. (g) Use RF machine learning models and filtered features to differentiate the DCA curves of SMI and NSM in the external verifying group. (h) Use RF machine learning models and filtered features to distinguish the AUC curves of SMI and NSM.

TABLE 2. AUC Comparison

Multimodal Vs T1COR	Multimodal Vs T2COR	Multimodal Vs T2AXI	Multimodal Vs T2SAG	Task
0.01	< 0.01	0.12	0.12	Train
0.04	0.28	0.03	< 0.01	Internal verification
0.80	0.85	0.90	0.94	External verification

CONCLUSION

Our research indicates that multimodal radiomics techniques using shoulder magnetic resonance imaging can effectively diagnose the presence of subscapularis injury.

ETHICAL APPROVAL

This retrospective study was approved by ethics committee of The Second Affiliated Hospital of Fujian Medical University(study no. IRB_2022.318). All methods were carried out in accordance with

relevant guidelines and regulations. Written informed consent was waived by the ethics committee of The Second Affiliated Hospital of Fujian Medical University. As this is a retrospective study, the patient's imaging data were desensitized before the study. Only the extracted feature area was retained as the original data, and no patient information was exposed. Therefore, after application, the informed consent form was not obtained.

CONTRIBUTIONS

HZX has conducted ROI outlining and is a major contributor to the conceptualization and composition of the manuscript. FKB provides code support and model building. LXC provides technical support. LYZ checks the ROI, XCH outlined the ROI related to ICC, and DZS reviewed and edited the manuscript. HNL, HXJ, CZK collected data. All authors have read and approved the final manuscript.

DISCLAIMER

The authors, their immediate families, and any research foundations with which they are affiliated have not received any financial payments or other benefits from any commercial entity related to the subject of this article.

INFORMED CONSENT

After our application, the informed consent was waived by the Ethics Committee of our hospital.

FUNDING

This manuscript was funded by the Qihang Project of Fujian Medical University (2022QH1128) and the Quanzhou Science and Technology Plan Project (2021N018S).

DATA AVAILABILITY

The datasets generated and/or analysed in this study are available from the corresponding author on reasonable request.

DECLARATION OF COMPETING INTEREST

The authors declare the following financial interests/personal relationships which may be considered as potential competing interests: Zhangsheng Dai reports statistical analysis and writing assistance were provided by The Second Affiliated Hospital of Fujian Medical University. If there are other authors, they declare that they have no known competing financial interests or personal relationships that could have appeared to influence the work reported in this paper.

REFERENCES

- Morag Y, Jamadar DA, Miller B, Dong Q, Jacobson JA. The subscapularis: anatomy, injury, and imaging. *Skeletal Radiol* 2011 Mar; 40(3):255–269. <https://doi.org/10.1007/s00256-009-0845-0>. Epub 2009 Dec 22. PMID: 20033149.
- Varacallo M, El Bitar Y, Sina RE, Mair SD. *Rotator Cuff Syndrome*. 2024 Mar 5. StatPearls [Internet]. Treasure Island (FL): StatPearls Publishing.; 2024 Jan. – PMID: 30285401.
- Endell D, Child C, Freislederer F, Moroder P, Scheibel M. Anatomie und Diagnostik von Subskapularissehnenrupturen [Anatomy and diagnostics of subscapularis tendon lesions]. *Unfallchirurgie* (Heidelberg) 2022 Aug; 125(8):647–658. <https://doi.org/10.1007/s00113-022-01207-7>. Epub 2022 Jul 11. PMID: 35819495.
- Yoon TH, Kim SJ, Choi YR, Cho JT, Chun YM. Arthroscopic revision rotator cuff repair: the role of previously neglected subscapularis tears. *Am J Sports Med* 2021 Dec; 49(14):3952–3958. <https://doi.org/10.1177/03635465211047485>. Epub 2021 Oct 15. PMID: 34652226.
- Huang EP, O'Connor JPB, McShane LM, et al. Criteria for the translation of radiomics into clinically useful tests. *Nat Rev Clin Oncol* 2023 Feb; 20(2):69–82. <https://doi.org/10.1038/s41571-022-00707-0>. Epub 2022 Nov 28.
- Yushkevich Paul A, Piven Joseph, Hazlett Heather Cody, et al. User-guided 3D active contour segmentation of anatomical structures: significantly improved efficiency and reliability. *Neuroimage* 2006 Jul 1; 31(3):1116–1128.
- Arevalillo JM, Navarro H. Exploring correlations in gene expression microarray data for maximum predictive-minimum redundancy biomarker selection and classification. *Comput Biol Med* 2013 Oct; 43(10):1437–1443.
- Demircioğlu A. Benchmarking feature selection methods in radiomics. *Invest Radiol* 2022 Jul 1; 57(7):433–443.
- Liu Y, Zhao H. Variable importance-weighted random forests. *Quant Biol* 2017 Dec; 5(4):338–351. Epub 2017 Nov 6. PMID: 30034909; PMCID: PMC6051549.
- Hu J, Szymczak S. A review on longitudinal data analysis with random forest. *Brief Bioinform* 2023 Mar 19; 24(2):bbad002<https://doi.org/10.1093/bib/bbad002>. PMID: 36653905; PMCID: PMC10025446.
- Vickers AJ, Cronin AM, Elkin EB, Gonen M. Extensions to decision curve analysis, a novel method for evaluating diagnostic tests, prediction models and molecular markers. *BMC Med Inform Decis Mak* 2008 Nov 26; 8:53. <https://doi.org/10.1186/1472-6947-8-53>. PMID: 19036144; PMCID: PMC2611975.
- Pruessner JC, Kirschbaum C, Meirlischmid G, Hellhammer DH. Two formulas for computation of the area under the curve represent measures of total hormone concentration versus time-dependent change. *Psychoneuroendocrinology* 2003 Oct; 28(7):916–931.
- DeLong ER, DeLong DM, Clarke-Pearson DL. Comparing the areas under two or more correlated receiver operating characteristic curves: a nonparametric approach. *Biometrics* 1988 Sep; 44(3):837–845.
- Alaia EF, Subhas N. Shoulder MR imaging and MR arthrography techniques: new advances. *Magn Reson Imaging Clin N Am* 2020 May; 28(2):153–163. <https://doi.org/10.1016/j.mric.2019.12.001>. Epub 2020 Feb 19. PMID: 32241655.
- Feldman MD. Editorial commentary: magnetic resonance imaging is generally superior to ultrasound for evaluation of rotator cuff pathology: if unrecognized subscapularis pathology is suspected after magnetic resonance imaging, ultrasound can then be performed. *Arthroscopy* 2022 Feb; 38(2):285–286. <https://doi.org/10.1016/j.arthro.2021.08.029>. PMID: 35123709.
- Adams CR, Brady PC, Koo SS, et al. A systematic approach for diagnosing subscapularis tendon tears with preoperative magnetic resonance imaging scans. *Arthroscopy* 2012 Nov; 28(11):1592–1600. <https://doi.org/10.1016/j.arthro.2012.04.142>. Epub 2012 Aug 24. PMID: 22922004.
- Velasquez Garcia A, Hsu KL, Marinakis K. Advancements in the diagnosis and management of rotator cuff tears. The role of artificial intelligence. *J Orthop*. 2023 Nov 8; 47:87–93. <https://doi.org/10.1016/j.jor.2023.11.011>. PMID: 38059047; PMCID: PMC10696306.